Research Article | Vol. 26, No. 12 | 11 Jun 2018 | OPTICS EXPRESS 15211
Optics EXPRESS

Si-based Mach-Zehnder wavelength/mode multi/demultiplexer for a WDM/MDM transmission system

S. OHTA,[1] T. FUJISAWA,[1,*] S. MAKINO,[1] T. SAKAMOTO,[2] T. MATSUI,[2] K. TSUJIKAWA,[2] K. NAKAJIMA,[2] AND K. SAITOH[1]

[1]*Graduate School of Information Science and Technology, Hokkaido University, North 14 West 9, Kita-ku, Sapporo, 060-0814, Japan*
[2]*NTT Access Network Service Systems Laboratories, NTT Corporation, 1-7-1 Hanabatake, Tsukuba-shi, Ibaraki, 305-0805, Japan*
**fujisawa@ist.hokudai.ac.jp*

Abstract: We propose and experimentally demonstrate a low-loss and low-crosstalk Mach-Zehnder mode/wavelength multi/demultiplexer for WDM/MDM transmission based on a Si-photonics platform. A broadband 3-dB mode divider, which is also newly devised here, makes it possible to compose a Mach-Zehnder filter for "mode" and "wavelength" simultaneously. Transmission characteristics of fabricated 3-dB mode dividers are in excellent agreement with theoretical results. Mach-Zehnder filters using the 3-dB mode divider with a free spectral range (FSR) of 20 and 1 nm are also fabricated and the modal crosstalk is less than −24 dB in the 40-nm wavelength range for the MZ filter with an FSR of 20 nm. The tuning of the peak wavelength position by the TiN heater is also demonstrated.

OCIS codes: (230.0230) Optical devices; (230.7370) Waveguides; (250.5300) Photonic integrated circuits.

References and links

1. Q. Xu, B. Schmidt, J. Shakya, and M. Lipson, "Cascaded silicon micro-ring modulators for WDM optical interconnection," Opt. Express **14**(20), 9431–9435 (2006).
2. Q. Fang, T. Y. Liow, J. F. Song, K. W. Ang, M. B. Yu, G. Q. Lo, and D. L. Kwong, "WDM multi-channel silicon photonic receiver with 320 Gbps data transmission capability," Opt. Express **18**(5), 5106–5113 (2010).
3. A. M. J. Koonen, H. Chen, H. P. A. van den Boom, and O. Raz, "Silicon photonic integrated mode multiplexer and demultiplexer," IEEE Photonics Technol. Lett. **24**(21), 1961–1964 (2012).
4. J. B. Driscoll, R. R. Grote, B. Souhan, J. I. Dadap, M. Lu, and R. M. Osgood, "Asymmetric Y junctions in silicon waveguides for on-chip mode-division multiplexing," Opt. Lett. **38**(11), 1854–1856 (2013).
5. J. Wang, S. He, and D. Dai, "On-chip silicon 8-channel hybrid (de)multiplexer enabling simultaneous mode- and polarization-division-multiplexing," Laser Photonics Rev. **8**(2), 18–22 (2014).
6. K. Saitoh, N. Hanzawa, T. Sakamoto, T. Fujisawa, Y. Yamashita, T. Matsui, K. Tsujikawa, and K. Nakajima, "PLC-based mode multi/demultiplexers for mode division multiplexing," Opt. Fiber Technol. **35**, 80–92 (2017).
7. Y. Yamashita, T. Fujisawa, S. Makino, N. Hanzawa, T. Sakamoto, T. Matsui, K. Tsujikawa, F. Yamamoto, K. Nakajima, and K. Saitoh, "Design and fabrication of broadband PLC-based 2-mode multi/demultiplexer using wavefront matching method," IEEE/OSA. J. Lightwave Technol. **35**(11), 2252–2258 (2017).
8. J. Wang, P. Chen, S. Chen, Y. Shi, and D. Dai, "Improved 8-channel silicon mode demultiplexer with grating polarizers," Opt. Express **22**(11), 12799–12807 (2014).
9. L. Han, S. Liang, J. Xu, L. Qiao, H. Zhu, and W. Wang, "Simultaneous wavelength- and mode-division (de)multiplexing for high-capacity on-chip data transmission link," IEEE Photonics J. **8**(2), 1–10 (2016).
10. L. W. Luo, N. Ophir, C. P. Chen, L. H. Gabrielli, C. B. Poitras, K. Bergmen, and M. Lipson, "WDM-compatible mode-division multiplexing on a silicon chip," Nat. Commun. **5**, 3069 (2014).
11. F. Horst, W. M. J. Green, S. Assefa, S. M. Shank, Y. A. Vlasov, and B. J. Offrein, "Cascaded Mach-Zehnder wavelength filters in silicon photonics for low loss and flat pass-band WDM (de-)multiplexing," Opt. Express **21**(10), 11652–11658 (2013).
12. T. Fujisawa, S. Kanazawa, Y. Ueda, W. Kobayashi, K. Takahata, A. Ohki, T. Ito, M. Kohtoku, and H. Ishii, "Low-loss cascaded Mach-Zehnder multiplexer integrated 25-Gbit/s × 4-lane EADFB laser array for future CFP4 100 GbE transmitter," IEEE J. Quantum Electron. **49**(12), 1001–1007 (2013).
13. K. Okamoto, *Fundamentals of Optical Waveguides* (Academic, 2000).
14. Z. Lu, H. Yun, Y. Wang, Z. Chen, F. Zhang, N. A. Jaeger, and L. Chrostowski, "Broadband silicon photonic directional coupler using asymmetric-waveguide based phase control," Opt. Express **23**(3), 3795–3806 (2015).

#327774 https://doi.org/10.1364/OE.26.015211
Journal © 2018 Received 5 Apr 2018; revised 23 May 2018; accepted 27 May 2018; published 31 May 2018

Optics EXPRESS

15. M. Shinkawa, N. Ishikura, Y. Hama, K. Suzuki, and T. Baba, "Nonlinear enhancement in photonic crystal slow light waveguides fabricated using CMOS-compatible process," Opt. Express **19**(22), 22208–22218 (2011).

1. Introduction

For the purpose of expanding communication capacity of optical communication system, wavelength division multiplexing (WDM) has been studied. However, there is a limit to the communication capacity expansion by WDM using single mode fiber. Therefore, a mode division multiplexing (MDM) has been studied for further expansion of communication capacity. WDM and MDM can be used simultaneously and make it possible to expand the network capacity further. For WDM and MDM, wavelength [1,2] and mode [3–10] multi/demultiplexers (MUX) are necessary. For the mode MUX, an asymmetric directional coupler (ADC) is often used [5–8]. The problem of ADC is that the loss and the modal crosstalk of ADC increase as the operation wavelength shifts from the center wavelength since ADC has parabolic spectral shape [6]. Therefore, when WDM and MDM are used in combination, the degradation of the optical signal for the wavelength far from the center will be large due to the large crosstalk. Therefore, broadband mode MUX is necessary for the combined use of WDM and MDM. These mode MUXes have been fabricated for various material platform, such as silica and Si. Among them, mode MUXes using Si-photonics platform [8–10] is promising due to its ultrasmall size. For WDM/MDM transmission MUXes based on Si waveguide, the multimode interference (MMI) type [9] and ring resonator type [10] mode MUX has been studied specially aimed for WDM/MDM transmission. For MMI type WDM/MDM mode MUX, the insertion loss is relatively high and wavelength dependence of MMI is large. For the ring resonator type WDM/MDM MUX, the position of the peak wavelength is very sensitive to the waveguide parameters. Mach-Zehnder (MZ) filters [11,12] are frequently used for single-mode WDM multiplexers, which is composed of two 3-dB coupler (usually, MMI waveguide) and delay line waveguides. The MZ filter has periodic transmission spectrum and the wavelength separation (free-spectral range: FSR) can be tuned by the length of the delay lines. If the MZ filter can be designed for mode MUX with periodical wavelength transmission as conventional single-mode MZ filter, it can work as broadband, low-loss, and low-crosstalk mode MUX for WDM/MDM transmission.

In this paper, we propose and experimentally demonstrate a novel MZ mode MUX based on Si waveguide for WDM/MDM transmission. The transmission spectrum of proposed MZ "mode" filter is periodic and at the peak wavelength, the loss and the crosstalk are small as in conventional MZ filter. To compose MZ mode MUX, a broadband 3-dB mode divider is necessary and the design methodology of 3-dB mode divider is also presented. The proposed 3-dB mode divider and the MZ mode MUX are fabricated in CMOS platform. Transmission characteristics of fabricated 3-dB mode dividers are in excellent agreement with theoretical results. For the MZ mode MUX, the devices with the FSR of 20 and 1 nm are fabricated and low-loss and low-crosstalk characteristics are presented. The modal crosstalk is less than –24 dB in 40-nm wavelength range for FSR 20-nm filter, which is more than two times compared with that of conventional ADC MUX. The tuning of the peak wavelength position by TiN heater is also demonstrated. These results indicate that the usefulness of the device for WDM/MDM transmission system.

2. The structure of proposed MZ mode multi/demultiplexer

Figure 1 shows the schematic of the MZ mode MUX proposed here. It consists of two 3-dB mode dividers and delay line waveguides. In the mode divider, input TE_0 mode from waveguide 2 is equally divided to TE_0 and TE_1 mode and TE_0 mode has additional phase delay in the delay line. Then, in the second mode divider, two modes are combined and outputted to either port depending on the phase difference. For conventional MZ filter, MMI is often used for 3-dB divider due to its broadband characteristics [12]. However, here, a

Optics EXPRESS

"mode" 3-dB divider is necessary as in Fig. 1, in which input TE_0 mode is equally divided to TE_0 and TE_1 modes in the broad wavelength range. Therefore, MMI cannot be used and different broadband 3-dB mode divider is necessary. Here, we also proposed broadband 3-dB mode divider using ADC with tapered waveguide. The design is performed by coupled-mode theory (CMT) [13] as shown in the next section.

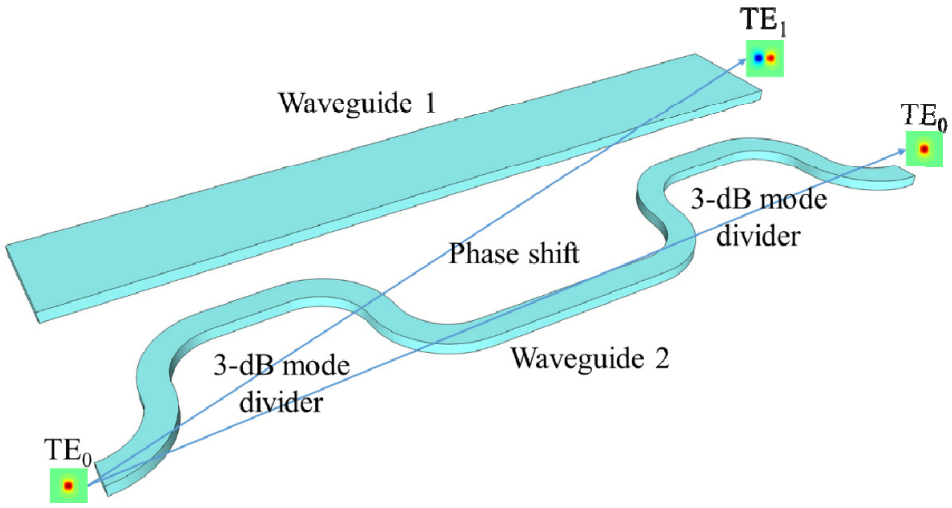

Fig. 1. The schematic of a MZ mode MUX.

3. 3-dB mode divider

Figure 2 shows a structure of the 3-dB mode divider based on tapered ADC. The waveguide widths of the waveguides 1 is w_1, the height of the waveguide is h, the spacing between the waveguides is g, and the coupling length is L_c. In the coupling region, the width of waveguide 2 is tapered from $w_2 - 2\Delta w$ to $w_2 + 2\Delta w$. The refractive index of the core is assumed to be 3.476 (silicon), and the refractive index of the cladding is assumed to be 1.444 (silica). First, we set the $w_1 = 818$ nm, $w_2 = 400$ nm, $g = 250$ nm and $h = 210$ nm. Therefore, we have to find optimum parameters of Δw and L_c. To determine Δw and L_c, following maximum deviation (MD) is evaluated [14], which is given by

$$MD = \max\left\{\left|T(\lambda)\right| - T_c\right\} \tag{1}$$

where $T(\lambda)$ is the transmission of TE_1 mode of port 3 at the wavelength $\lambda = 1500$, 1525, 1550, 1575, and 1600 nm when the TE_0 mode is launched from port 2, and T_c is the reference transmission. Here, $T_c = 0.5$ because we want to design 3-dB mode divider. The transmission is calculated by CMT. We calculated the effective refractive indexes of Si-wire waveguides for various widths by using finite-element method and use them for the input for solving coupled mode equation. Figure 3 shows the MD as a function of Δw and L_c, the white dot in the figure is the point where the MD is the minimum. From the figure, the broadband operation can be expected by choosing $\Delta w = 11$ nm and $L_c = 27$ μm. Figure 4 (a) shows the calculated transmission spectra of the 3-dB mode divider. Green and red lines show the transmission of the conventional ADC divider and the designed 3-dB mode divider. Here, the conventional ADC divider is composed of two straight waveguides 1 and 2 ($\Delta w = 0$ nm, $w_1 = 837$ nm, $w_2 = 400$ nm, $g = 200$ nm) and $L_c = 9.09$ μm, which is the half of coupling length at 1.55 μm. Hereafter, we call this structure as "straight divider". The designed 3-dB mode divider has a transmission of about −3 dB over the wavelength of 1530 to 1600 nm, while the transmission of the straight divider deviates from −3 dB for the wavelength far from 1.55 μm.

Optics EXPRESS

Figure 4 (b) shows the transmission of the mode divider as a function of waveguide width variation for 1500, 1550, and 1600 nm. ± 10 nm waveguide width variation is assumed for waveguides 1 and 2. Green region corresponds to the transmission around 0.5. From the Figure, if the deviations for w_1 and w_2 are similar, the transmission is not so changed from 0.5.

We fabricated designed 3-dB mode divider using a CMOS process and measured the transmission spectra to confirm the broadband characteristics. Figure 5 shows a micrograph of the fabricated 3-dB mode divider based on tapered waveguide. Figure 6 shows the measurement setup. TE-polarized light from ASE light source is coupled to the chip through inverse taper spot size converter [15] fabricated at the both edges of the chip. Transmitted light is received by optical spectrum analyzer. The transmission is measured by subtracting the transmitted power through a reference straight waveguide fabricated in the same chip from the transmitted power through the device. For the measurement of the TE_1 mode transmission, as shown in Fig. 5 (bottom), we fabricated two-cascaded 3-dB mode divider and measurement was done by that structure. By using this configuration, we can measure the transmission of TE_1 mode by TE_0 mode [port2 to port4 in Fig. 5 (bottom)], which is much easier. Figure 7 shows the measured transmission spectra of the fabricated 3-dB mode divider. Green and red lines show the transmission spectra of the straight divider and the 3-dB mode divider with tapered waveguide. From Fig. 4 and 7, the calculated results and the measured results are in very good agreement. In the case of the straight divider, the port imbalance is increased for the wavelength far from the center (around 1540 nm). On the other hand, the transmission of the designed mode divider is around −3 dB and the port imbalance is less than −0.7 dB from 1530 to 1600 nm, showing the broadband 3-dB mode dividing operation.

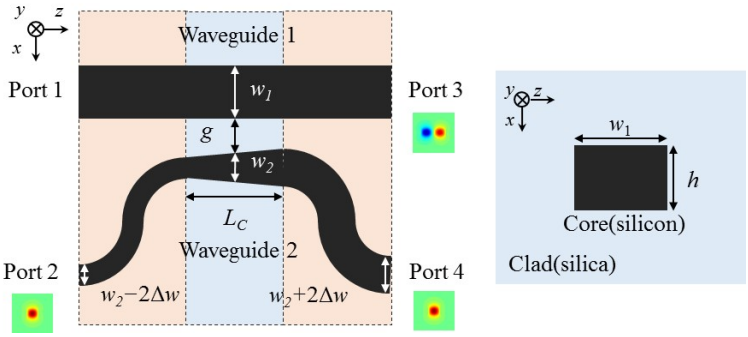

Fig. 2. The schematic of the 3-dB mode divider based on tapered ADC (left) top-view and (right) the cross section of the waveguide 1.

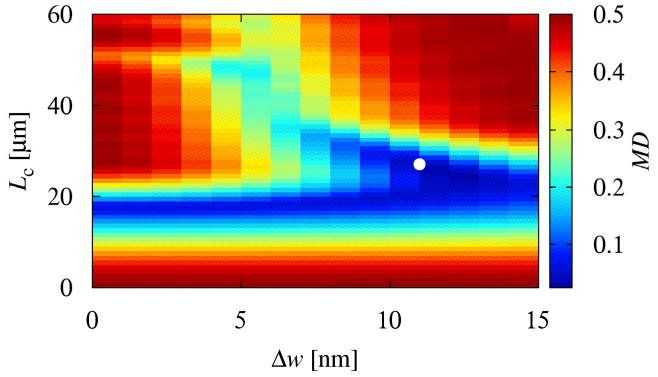

Fig. 3. *MD* as a function of L_c and Δ*w*.

Optics EXPRESS

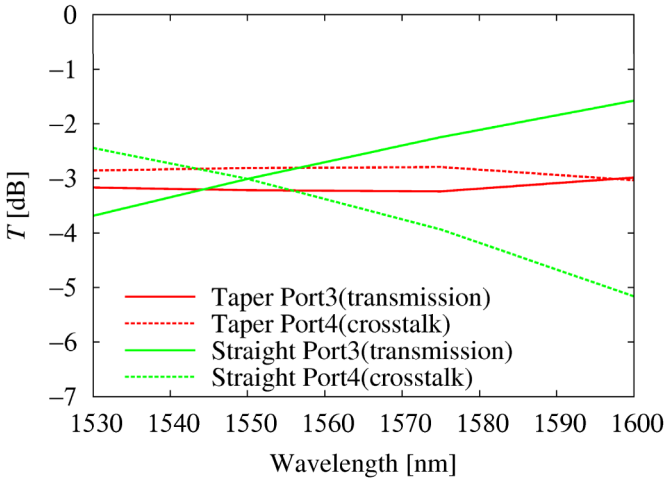

(a)

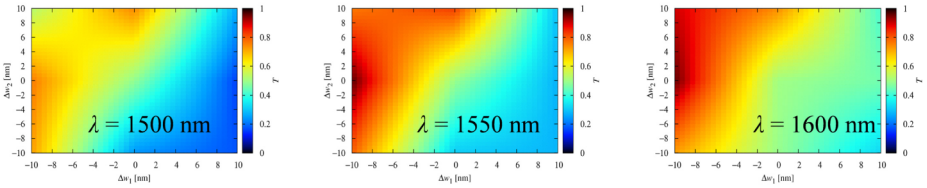

(b)

Fig. 4. (a) The calculated transmission spectra of the 3-dB mode divider and (b) the fabrication tolerance of the mode divider for 1500, 1550, and 1600 nm.

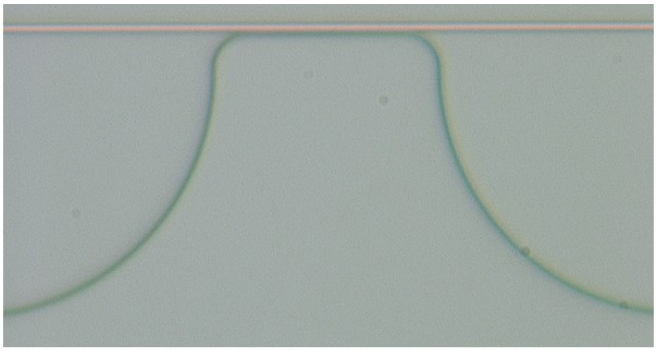

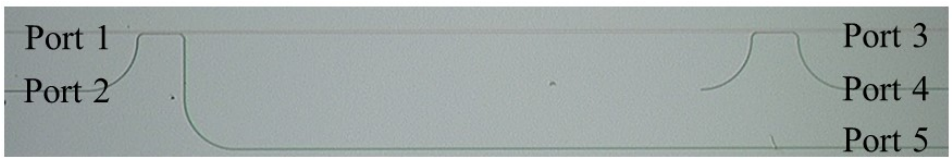

Fig. 5. The micrograph of (top) the fabricated 3-dB mode divider based on tapered waveguide and (bottom) two-cascaded 3-dB mode divider.

Optics EXPRESS

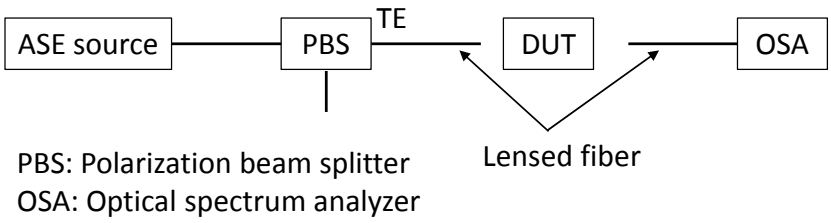

Fig. 6. The measurement setup.

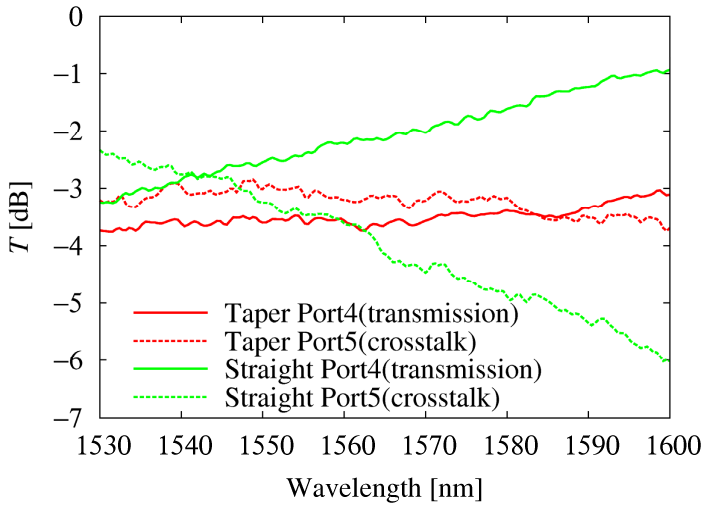

Fig. 7. The measured transmission spectra of the fabricated 3-dB mode divider.

4. Mach-Zehnder mode multi/demultiplexer

Figure 8 shows the schematic of the MZ mode MUX. In the 3-dB mode divider region, the parameters are the same with the previous section. The values of the parameters are w_1 = 818 nm, w_2 = 400 nm, Δw = 11 nm, g = 250 nm, h = 210 nm, L_c = 27 μm. L_1 and L_2 are the length of delay line waveguides. In the MZ filter, a peak of the transmission appears periodically with respect to the wavelength by providing an optical path difference between the two arm waveguides. We can obtain arbitrary FSR by adjusting the length of the delay line. FSR is given by

$$\Delta\lambda = \frac{\lambda^2}{\left| N_1\left(L_1 + 2L_c\right) - N_2\left(L_2 + 2L_c\right)\right|} \tag{2}$$

Here, N_1 and N_2 are the group indices of TE_1 and TE_0 modes in the waveguides 1 and 2. It is possible to design an MZ mode MUX having an arbitrary FSR by using Eq. (2). When calculating transmission spectra by CMT, strictly speaking, N_2 in the coupling region is changed due to the taper and it should be taken into account. However, for simplicity, N_2 in the coupling region is approximated to the value of the waveguide with the width of $w_2 + 2\Delta w$ (same as the delay line waveguide). Therefore, the calculated group indices are N_1 = 4.415 for w_1 = 818 nm and N_2 = 4.186 for $w_2 + 2\Delta w$ = 422 nm. From Eq. (2), L_1 = 20.0 μm and L_2 = 52.74 μm for $\Delta\lambda$ = 20 nm (coarse WDM grid). Figure 9 shows the transmission spectra of the MZ mode MUX with $\Delta\lambda$ = 20 nm calculated by CMT. Solid and dashed lines in Fig. 9 show the calculated transmission (port2 to port3) and crosstalk (port2 to port4) spectra. The red and green lines show the spectra of MZ mode MUX with $\Delta\lambda$ = 20 nm and conventional ADC

Optics EXPRESS

MUX. Here, the schematic of the conventional ADC is the same as the mode divider, namely, it is shown in Fig. 2. The conventional ADC has two straight waveguides in the coupling region without taper and L_c is set to the coupling length at 1550 nm. The parameters of the conventional ADC are w_1 = 837 nm, w_2 = 400 nm, Δw = 0 nm, g = 200 nm, and L_c = 18.18 μm [see Fig. 2 for each parameter]. From Fig. 9, periodic transmission spectra peculiar to the MZ filter is obtained for the MZ mode MUX. On the other hand, for the conventional ADC MUX, the crosstalk becomes worse for the wavelength far from the center wavelength. For the proposed MZ mode MUX, low-loss and low-crosstalk characteristics are obtained in the broad wavelength range, showing the advantage of MZ mode MUX for WDM/MDM transmission.

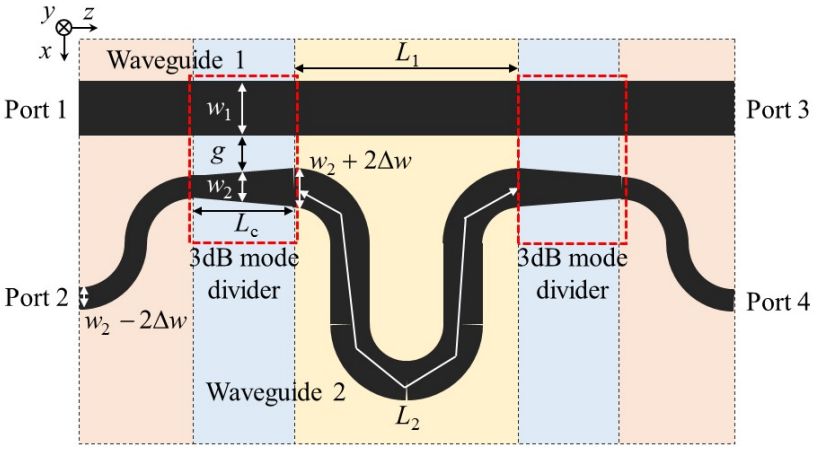

Fig. 8. The schematic of the MZ mode MUX.

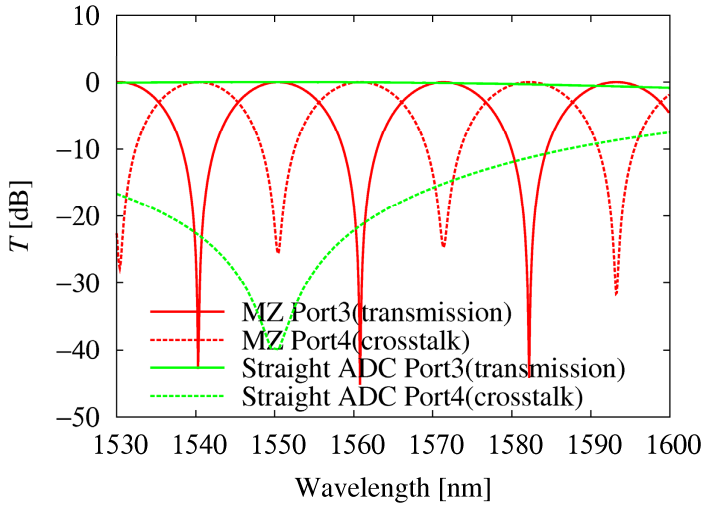

Fig. 9. The transmission spectra of the MZ mode MUX with Δλ = 20 nm calculated by CMT.

Subsequently, the transmission spectra of the MZ mode MUX fabricated by CMOS process is measured. Figure 10 shows a micrograph of the fabricated MZ mode MUX. The measurement is done in the same way as the measurement of the 3-dB mode divider in the previous section. Figure 11 shows the measured transmission spectra of the fabricated MZ mode MUX with FSR = 20 nm and conventional ADC. The red and green lines show the spectra of MZ mode MUX with Δλ = 20 nm and conventional ADC MUX. Solid and dashed

lines show the transmission (port2 to port4) and crosstalk (port2 to port5) spectra of the MZ mode MUX and conventional ADC MUX. From Fig. 11, for the conventional ADC, parabolic transmission spectra are obtained as expected. However, the crosstalk of the fabricated conventional ADC MUX is significantly worse than calculated and we believe that this is due to the fabrication imperfection. Therefore, we compare the transmission spectra between calculated results of the conventional ADC MUX and measured results of the MZ mode MUX, which is more severe comparison for MZ mode MUX. For the MZ mode MUX, periodic spectra are obtained, and the FSR is about 20 nm. The wavelength range, in which the crosstalk is less than −24 dB, is about 16 nm for the conventional ADC MUX from Fig. 9. For the MZ mode MUX, the wavelength range for the crosstalk < −24 dB is more than 40 nm from Fig. 11 (we can only measure the crosstalk of only two FSR bandwidth in the wavelength range of our lightsource (1530 to 1600 nm)), which is two times larger than that of the conventional ADC MUX.

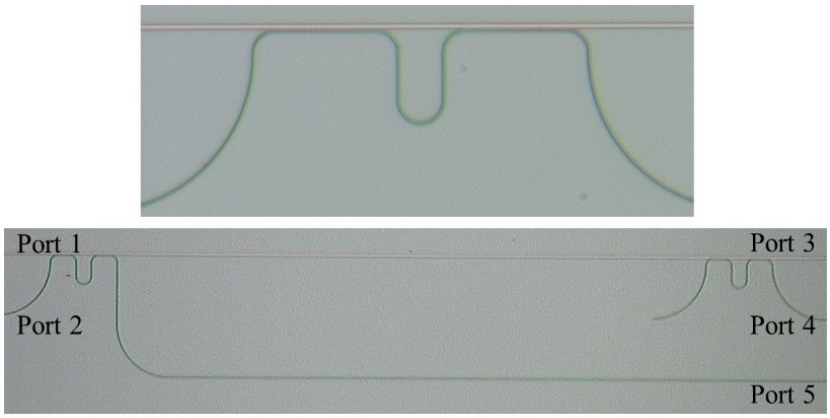

Fig. 10. Micrograph of (top) the fabricated MZ mode MUX and (bottom) two-cascaded MZ mode MUX.

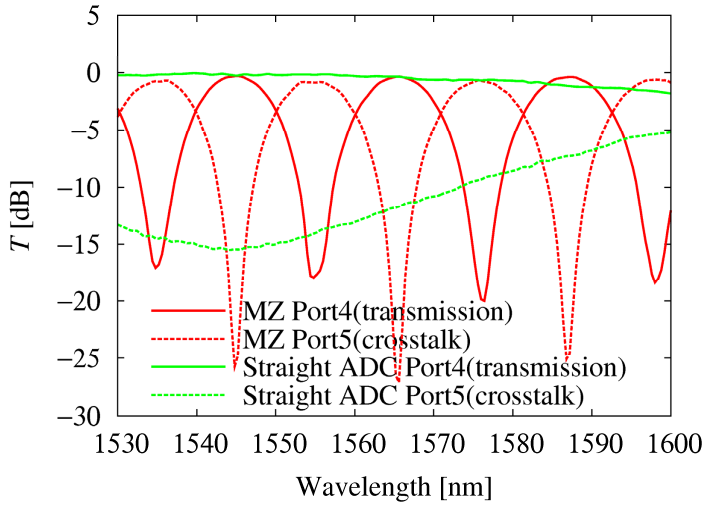

Fig. 11. The measured transmission spectra of the fabricated MZ mode MUX with FSR = 20 nm.

We fabricated and measured the MZ mode MUX using conventional straight 3-dB mode divider to prove the need for a broadband 3-dB mode divider. Figure 12 shows the measured

Optics EXPRESS

transmission spectra of the fabricated MZ mode MUX using the straight divider. $\Delta\lambda$ is set to 20 nm. From Fig. 12, expected FSR is also obtained for MZ mode MUX with the straight divider, like Fig. 11. However, the loss and crosstalk of straight MZ at peak wavelength are increased for the wavelength far from the center (around 1545 nm). This is because that the mode splitting ratio of the straight divider deviates from −3 dB as shown in Fig. 7. Therefore, designed 3-dB mode divider is indispensable to compose broadband MZ filter.

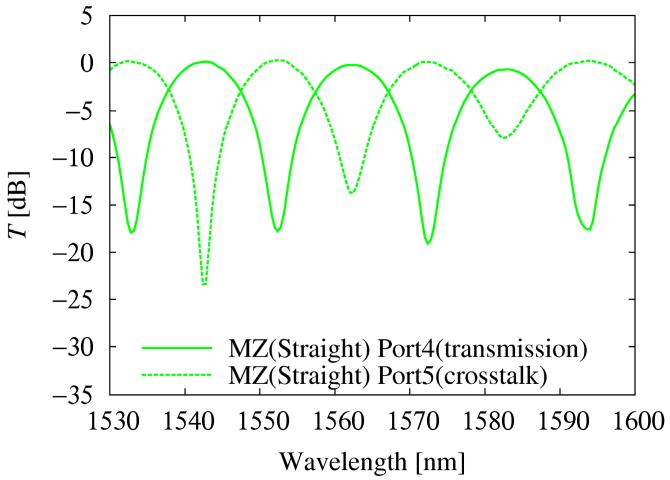

Fig. 12. The measured transmission spectra of the fabricated MZ mode MUX with straight divider.

Next, we show that FSR can be changed by adjusting the length of the delay line. Assuming L_1 = 20 μm as in the case of FSR = 20 nm, FSR = 1 nm if L_2 = 597.9 μm from Eq. (2). Figure 12 shows the measured transmission spectra of the fabricated MZ mode MUX with FSR = 1 nm. It can be seen from Fig. 13 that there are two bottom peaks for transmission to Port 4. This is because that it receives light, which passing through two MZ mode MUX and the peak wavelengths of the first and second MZ mode MUX are slightly changed because of the fabrication error. FSR is about 1 nm as expected. From this result, FSR can be freely designed by using Eq. (2).

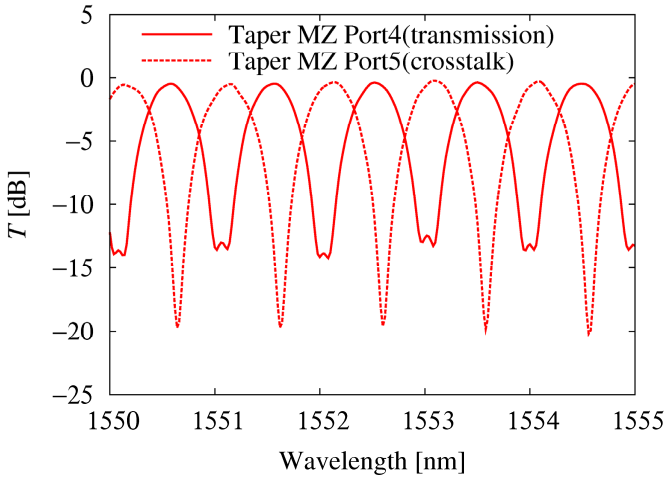

Fig. 13. The measured transmission spectra of the fabricated MZ mode MUX with FSR = 1 nm.

Optics EXPRESS

Finally, the tunability of the filter peak wavelength by using a heater is demonstrated. Figure 14 shows a micrograph of MZ mode MUX with FSR of 1 nm. TiN heater is added on top of the delay line waveguide 2. The width, thickness, and length of the heater on top of the waveguide2 are 4 μm, 120 nm, and 135 μm. The separation between the heater and the top of the waveguide is larger than 1.2 μm. A heat isolation trench is added to enhance the heating efficiency. Figure 15 shows the measured transmission spectra of MZ mode MUX with the heater for different injection current. The position of the peak wavelength of the transmission spectra is shifted to the longer wavelength side as the injection current to the heater is increased. From this result, the peak wavelength can be tuned by the heater.

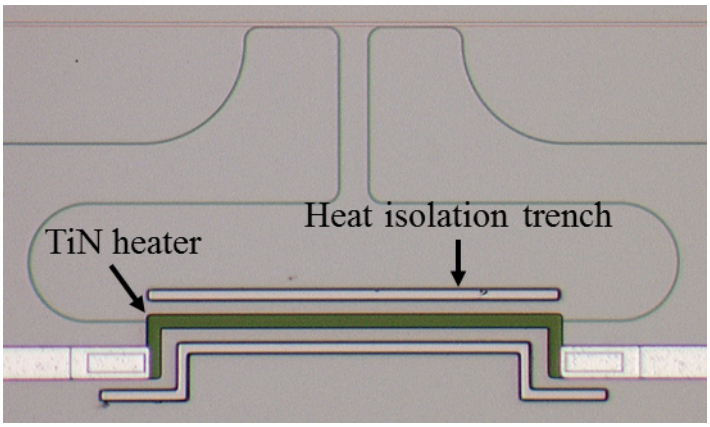

Fig. 14. Micrograph of the fabricated MZ mode MUX with heater in the delay line waveguide 2.

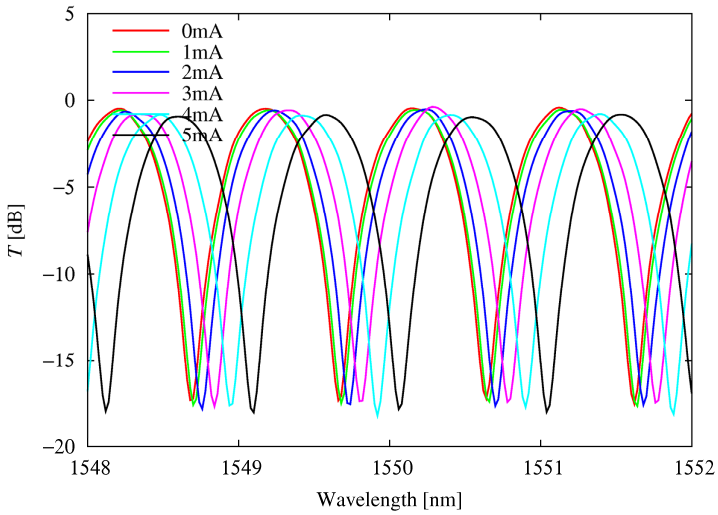

Fig. 15. The measured transmission spectra of the MZ mode MUX with the heater.

5. Conclusion

A novel mode MUX based on MZ filter was proposed for the combined use of WDM and MDM transmission. A newly designed broadband 3-dB mode divider makes it possible to compose broadband MZ "mode" filter. Both the 3-dB mode divider and the MZ mode MUX were fabricated in CMOS platform and measured results are in excellent agreement with the theory. The fabricated device exhibits low-loss and low-crosstalk characteristics in the broad wavelength range and is useful for WDM/MDM transmission.